Self-absorption of heliumlike satellite lines in high-density fusion plasmas

D. Duston* and J. Davis
Plasma Radiation Group, Plasma Physics Division, Naval Research Laboratory, Washington, D. C. 20375
(Received 14 September 1979)

The high densities obtained in recent laser fusion experiments have created a need for additional plasma density diagnostics. The ratio of two heliumlike satellite lines, the $1s2p\,^3P \rightarrow 2p\,^2\,^3P$ and $1s2s\,^3S \rightarrow 2s2p\,^3P$ transitions, has shown promise as a spectral diagnostic when laser-imploded microballoons are seeded with medium-atomic-weight gases. In this study results are presented from a collisional-radiative ionization-dynamics model with photoexcitation processes included that indicate that the emission from these satellite lines is strongly affected by opacity in density and temperature regimes common to plasmas to which this diagnostic could be applied effectively. The radiation emission attenuated by photon reabsorption is presented for neon, aluminum, and argon plasmas and compared with results predicted when the calculation is undertaken in an optically-thin-plasma approximation. The opacity effects are seen to cause multivaluedness in the line ratio at several temperatures, and an overall loss of sensitivity of the ratio with density is predicted.

In recent years much work has been devoted to understanding radiation spectra emitted from dense high-temperature plasmas. Although most of the available experimental spectra have been obtained in the past from laser-produced plasmas,[1] exploding wire plasmas,[2] or gas-puff Z pinches,[3] data have recently been obtained by seeding glass microballoons with a medium-Z gas to produce x rays from bound-bound transitions occurring during a high-temperature compression of an imploded pellet.[4,5] The purpose of these experiments is to make full use of the x-ray lines as diagnostic indicators of the temperature and density history of the plasma contained by the laser-imploded glass shell. Unfortunately, the densities being attained at present, typically 10^{22}–10^{23} electrons per cubic centimeter, are in a somewhat difficult regime for their determination. Several techniques are available to the experimentalist, e.g., Stark broadening of selected lines,[6] merging of the series limit,[7] and such selected line-intensity ratios as the intercombination-to-resonance line ratio in heliumlike ions.[8] In the past, these techniques have been applied to laboratory plasmas under the assumption that these lines are optically thin. However, the validity of the density determinations strongly depends on whether these high-density plasmas are indeed optically thin and, if not, whether opacity effects vitiate their usefulness as density diagnostics.

In this paper, a study is made of the radiation emitted by two doubly excited levels of the heliumlike ion which show up as satellite lines to the hydrogenlike resonance line, and the line ratio formed by them as used to determine the plasma density. The sensitivity range of this diagnostic extends over several orders of magnitude in ion density, but is centered at approximately 10^{21} ions/cm^3 for materials presently used for microballoon seeding, making it a logical candidate for application in density determinations of compressed-laser-pellet experiments. A theoretical calculation of this line emission as it is generated in optically thin neon, aluminum, and argon plasmas is performed. In addition, this line emission is also calculated in plasmas where photo excitation is at least equally important as collisional excitation in order to assess the effect of opacity on the line-intensity ratio at high density.

I. THEORETICAL MODEL

It has been shown from recent work[9,10] that, in the optically thin approximation, the line ratio under consideration is independent of the hydrogenlike ground-state population and depends only on the electron density, electron temperature, and atomic parameters associated with the levels being studied. We define an abbreviated level structure as shown in Fig. 1, and analytically calculate the line ratio in terms of the populations of the two doubly excited states of the heliumlike ion, the $2s2p\,^3P$ and $2p^2\,^3P$ levels, and their radiative transitions, $1s2s\,^3S \rightarrow 2s2p\,^3P$ and $1s2p\,^3P \rightarrow 2p^2\,^3P$.

First, the atomic rate equations for each of the doubly excited states are written

$$\frac{dN_1}{dt} = C_1 N_e N_g + Y N_e N_2 - (\Gamma_1 + A_1 + X N_e) N_1 ,$$
$$\frac{dN_2}{dt} = C_2 N_e N_g + X N_e N_1 - (\Gamma_2 + A_2 + Y N_e) N_2 . \quad (1)$$

Here, N denotes the state density, C is the electron-capture rate coefficient, Γ is the autoioni-

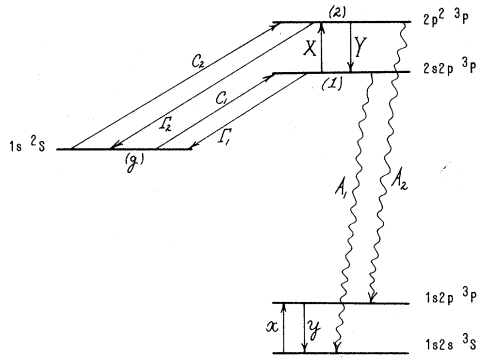

FIG. 1. Simplified level structure for analytic treatment of the satellite line emission from heliumlike ions.

zation rate, A is the spontaneous decay rate, X is the electron-excitation rate coefficient, Y is the deexcitation rate coefficient, N_e is electron density, and the subscripts g, 1, and 2 indicate the $1s$, $2s2p$, and $2p^2$ states, respectively. Note that at the densities under consideration here, the electron and ion collisional rates coupling the individual j components of each of the two doubly excited levels are sufficiently large that it is assumed that they will each be populated according to their statistical weights, allowing for their representation as the two n levels in Fig. 1 (the j degeneracy has been removed). Under the assumption that the atomic rates are faster than the typical hydrodynamic time scale of the plasma [collisional-radiative equilibrium (CRE) model], the time derivatives in Eq. (1) are set to zero and the solutions for N_1 and N_2 are given by

$$N_2 = \frac{N_1\theta_1 - N_g N_e C_1}{N_e Y},$$
$$N_1 = \frac{N_g N_e^2 C_2 Y + N_g N_e C_1 \theta_2}{\theta_1\theta_2 - N_e^2 X Y}, \tag{2}$$

where $\theta_1 = A_1 + \Gamma_1 + XN_e$ and $\theta_2 = A_2 + \Gamma_2 + YN_e$. The line intensity is now given by $NA\Delta E$, where ΔE is the transition energy. Forming the line ratio and solving from Eq. (2), one can readily show that

$$R = \frac{N_2 A_2 \Delta E_2}{N_1 A_1 \Delta E_1} = \frac{A_2\Delta E_2}{A_1\Delta E_1}\frac{1}{YN_e} \times\left(\theta_1 - \frac{\theta_1\theta_2 - XYN_e^2}{YN_e(C_1/C_2)+\theta_2}\right) \tag{3}$$

and hence the ratio is independent of N_g.

For this study, we have chosen to use the radiative decay and autoionization rates of Vainshtein and Safronova[11] and average over the individual j components so as to be applicable to our model. The electron-capture rate coefficient is obtained by detailed balance of the autoionization rate, giving, for example, for state 2,

$$C_2 = \Gamma_2 (g_2/2g_g)(2\pi\hbar^2/m_e kT_e)^{3/2} e^{-E_s/T_e}, \tag{4}$$

where g is the statistical weight and E_s is the energy of the doubly excited state above that of the hydrogenlike ground state. The electron collisional excitation rate coefficient coupling the two levels has been calculated by the method of distorted waves,[12] and the deexcitation rate coefficient also obtained from detailed balance of the excitation rate coefficient

$$Y = X(g_1/g_2)e^{\Delta E/T_e}, \tag{5}$$

where ΔE is the energy separation of the two doubly excited states.

As a theoretical check on the calculation, approximations can be made in Eq. (3) to obtain the values for the ratio in the local thermodynamic equilibrium (LTE)[13] and corona limits.[14] In the LTE (high-density) limit, it is expected that collisional rates will dominate over competing radiative rates. Setting the A's and Γ's to zero in the large parentheses in Eq. (3), we obtain the LTE limit (noting that $g_1 = g_2$),

$$R_{\rm LTE} = \frac{A_2\Delta E_2}{A_1\Delta E_1}\frac{X}{Y} = \frac{A_2\Delta E_2}{A_1\Delta E_1}e^{-\Delta E/T_e}. \tag{6}$$

In the corona limit, radiative processes are dominant over competing collisional rates. If we form the ratio N_2/N_1 from Eq. (2) and let θ_1 go to $\alpha_1 = A_1 + \Gamma_1$ and θ_2 go to $\alpha_2 = A_2 + \Gamma_2$, we get

$$\frac{N_2}{N_1} \cong \frac{\alpha_1}{N_e Y} - \frac{C_1}{Y}\frac{\alpha_1\alpha_2 - N_e^2 XY}{N_e^2 C_2 Y + N_e C_1 \alpha_2}. \tag{7}$$

Ignoring the $N_e^2 XY$ term in the numerator, factoring out an $\alpha_1/N_e Y$ term from the bracket, combining, and expanding out, assuming that $C_1\alpha_2 \gg N_e C_2 Y$, we obtain the following expression in the corona limit:

$$R_{\rm cor} \simeq \frac{A_2\Delta E_2}{A_1\Delta E_1}\frac{\Gamma_2(A_1+\Gamma_1)}{\Gamma_1(A_2+\Gamma_2)}e^{-\Delta E/T_e}, \tag{8}$$

where we have eliminated C_1/C_2 using Eq. (4). It is expected that Eq. (6) and (8) will define the high- and low-density limits of the optically thin line ratios studied here; comparisons will be made in Sec. III.

II. IONIZATION-RADIATION MODEL

In Sec. I, it was determined that the $1s2p\,^3P \rightarrow 2p^2\,^3P$ to $1s2s\,^3S \rightarrow 2s2p\,^3P$ line-intensity ratio was independent of the populations of surrounding ground or singly excited levels. If opacity effects are included in the model, this is not the

case. When the optical depths of the two satellite lines exceed 1, photoexcitation is expected to significantly affect the populations of the doubly excited states, coupling them to the lower states of the satellite-line transitions, the $1s2s\,^3S$ and $1s2p\,^3P$ levels. Although previous authors[9,10] have discounted radiative absorption processes in forming this ratio with the argument that the lower states of the lines are excited states of the heliumlike ion and are expected to be well down in population from the ground state, and hence generate small optical depths for these lines, we have found this not to be the case at densities and temperatures where the line ratio is expected to be a valuable diagnostic. Hence some means must be included in the calculation to take account of radiative transfer and photoexcitation when the satellite lines become optically thick.

As a basis for these calculations, we use an atomic model based on rate equations describing the processes populating ground states and selected excited states for each element studied. The processes in this model include collisional ionization; collisional, radiative, and dielectronic recombination; collisional excitation; collisional and spontaneous radiative deexcitation; and stimulated absorption and emission. The equations are solved time independently for a homogeneous plasma of constant electron temperature and ion density to yield fractional populations of the states, electron density, and line-emission intensities self-consistently with the radiation-transport calculations.

The photon-absorption processes are taken into account by a phenomenological frequency-diffusion model which allows an emitted photon to escape an absorbing plasma by successive collisions with ions, eventually scattering into the optically thin wings of a broadened line profile and escaping the plasma. A photon-trapping factor can be calculated as a function of the optical depth through the plasma at a frequency corresponding to the line-center frequency of the photon transition. This factor can thus reduce the line source function depending on the opacity of the plasma. It is also included in the rate equations to allow for the optical pumping of the upper levels of thick lines. The optical depth of the line is defined as

$$\tau_\nu = \frac{\pi e^2}{m_e c} f_{jk} \frac{\bar{L}}{\sqrt{\pi}} \frac{N_j}{\Delta\nu_D} \varphi(\nu), \tag{9}$$

where the Doppler width is given by

$$\Delta\nu_D = (2T_i/Mc^2)^{1/2}\nu_0 . \tag{10}$$

Here, f is the dipole oscillator strength, $\bar{L}$ is the effective photon path length through the plasma, N_j is the lower-state population, φ is the line profile function, T_i is ion temperature, and M is the ion mass. In order to accurately determine the N_j's and hence, the optical depths, a number of excited states were included in the atomic model in addition to all the ground states: the $n=2,3,4,5$ levels in the hydrogenlike ion, the $2s\,^1S, 2s\,^3S, 2p\,^1P, 2p\,^3P$, 3-singlet, 4-singlet, and 5-singlet levels in the heliumlike ion, and the $2p, 3s, 3p, 3d$, and $4d$ levels in the lithiumlike ion. A complete discussion of the method of calculating rate coefficients, atomic structure, and the opacity model has been presented in previous studies.[15,16]

III. RESULTS

A. Optically thin approximation

In order to obtain a clear understanding of the role played by collisions in determining this intensity ratio, and also to compare our predictions with previous work, an initial study of the formation of the level populations in the optically thin approximation was undertaken. Hence no reabsorption of photons and subsequent optical pumping was allowed in obtaining these first calculations. Since it has been shown in Sec. II that the line ratio is independent of all but the $2s2p$ and $2p^2$ populations in an optically thin plasma, the results are merely the solution to Eq. (3). The ratio is depicted graphically in Figs. 2–4 for neon, aluminum, and argon plasmas, shown at various temperatures over a wide range of ion densities. As can be seen from the figures, each plasma produces the same basic behavior in the line ratio: a relatively constant low- and high-density limit, connected by a rapidly ascending transition region over which the ratio provides its diagnostically valuable density dependence.

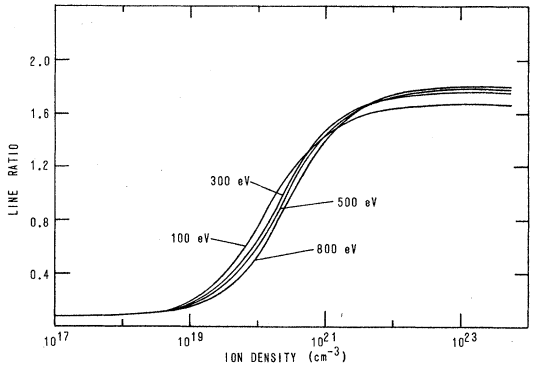

FIG. 2. $(1s2p\,^3P \rightarrow 2p^2\,^3P)/(1s2s\,^3S \rightarrow 2s2p\,^3P)$ intensity ratio for a neon plasma in the optically thin approximation.

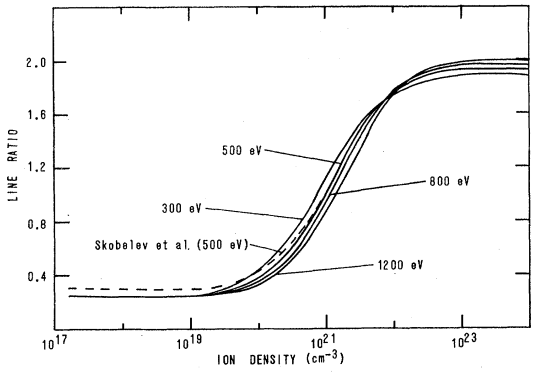

FIG. 3. $(1s2p\,^3P \rightarrow 2p^2\,^3P)/(1s2s\,^3S \rightarrow 2s2p\,^3P)$ intensity ratio for an aluminum plasma in the optically thin approximation.

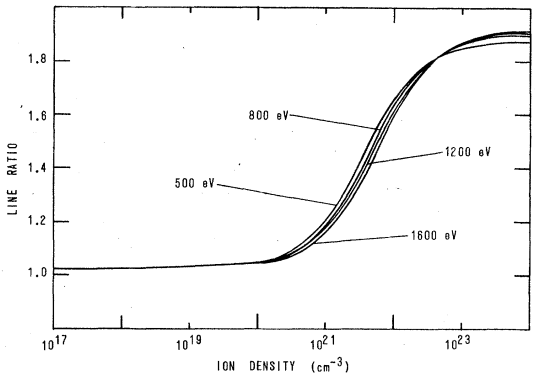

FIG. 4. $(1s2p\,^3P \rightarrow 2p^2\,^3P)/(1s2s\,^3S \rightarrow 2s2p\,^3P)$ intensity ratio for an argon plasma in the optically thin approximation.

The $2s2p$ level is preferentially populated over the $2p^2$ level at low densities since the ratio of the radiative decay rate to the autoionization rate for the $2s2p$ state is smaller than that of the $2p^2$ state. However, the electron collisions coupling these two states become increasingly important in the redistribution of the populations as the plasma electron density increases, resulting in an increase in the $2p^2$ level relative to the $2s2p$ level and a corresponding increase in the line-intensity ratio. Finally, in the high-density limit, the two levels reach a state of statistical equilibrium relative to each other with the population ratio given by $e^{-\Delta E/T_e}$ and the line ratio given by Eq. (6).

Note that for purposes of density diagnostics in laser-imploded pellets doped with a small amount of neon, the most effective region for density predictions is from 3×10^{19} to 3×10^{21} ions/cm^3, while for argon-seeded pellets, the region is from 5×10^{20} to 5×10^{22} ions/cm^3. Thus, with the appropriate gas doping, it is conceivable that this technique would be an effective diagnostic over three orders of magnitude in density, provided the pellet fuel can be heated sufficiently to attain temperatures where the satellite-line emission is intense enough to be measured.

Also shown in Fig. 3 are the results of an earlier work by Vinogradov *et al.*[9] The model used in Ref. 9 leading to their predicted line ratio was applied to an aluminum plasma and the ratio calculated for an electron temperature of 500 eV. In fact, Ref. 9 includes only the emission from four transitions in the $2p^2$-$1s2p$ manifold ($^3P_2$-$^3P_2$, $^3P_2$-$^3P_1$, $^3P_1$-$^3P_1$, $^3P_1$-$^3P_0$) for experimental reasons, while our calculation includes all six of the components (the $^3P_1$-$^3P_2$ and $^3P_0$-$^3P_1$ in addition to the four above) from the $2p^2$ state. The curve reflects the calculation from Ref. 9, however, with all six lines included, and is seen to be in excellent agreement with our CRE model predictions.

In order to verify that our calculations approach

TABLE I. Atomic parameters used in the collisional radiative model to analyze the heliumlike satellite-line structure.

Parameter	Neon	Aluminum	Argon
λ_1 (Å)	12.307	7.252	3.763
λ_2 (Å)	12.323	7.26	3.766
ΔE_1 (eV)	1007.4	1709.6	3294.56
ΔE_2 (eV)	1006.1	1707.8	3292.46
ΔE (eV)	8.64	11.7	18.74
f_1	0.3935	0.3974	0.4036
f_2	0.2390	0.2657	0.2639
A_1 (sec^{-1})	5.776×10^{12}	1.68×10^{13}	6.347×10^{13}
A_2 (sec^{-1})	1.05×10^{13}	3.362×10^{13}	1.241×10^{14}
Γ_1 (sec^{-1})	1.353×10^{13}	1.357×10^{13}	1.387×10^{13}
Γ_2 (sec^{-1})	4.287×10^{11}	1.987×10^{12}	1.352×10^{13}
R_{LTE} (500 eV)	1.78	1.953	1.885
R_{cor} (500 eV)	0.100	0.244	1.031

the correct limits, the values for the satellite-line ratio in the LTE and corona approximations were determined in accordance with the parameters given in Table I and Eqs. (6) and (8). Comparison between the values obtained in Table I at electron temperatures of 500 eV and Figs. 2–4 generated by our model also indicates good agreement.

B. Optically thick plasma

At low plasma densities, optical depths of emission lines are small, as defined by Eq. (9), and, consequently, the photon-absorption effects are small relative to competing collisional and spontaneous radiative rates and can be neglected. As the plasma density increases, the photoexcitation rates become comparable or even exceed competing processes, resulting in significant changes in the population densities of the excited states and the subsequent bound-bound radiation emission from these levels. In previous studies, the effects of these processes on the determination of the hydrogenlike satellite-line ratio have been ignored with the justification that the lower state of each of the relevant transitions is itself an excited level, and hence the populations of these levels should not be large enough in the density range of interest to contribute to a large optical depth in plasmas of the physical dimensions commonly encountered in the laboratory.

In order to test the validity of this assumption, we performed calculations of the line ratio using our radiation-ionization dynamics model with frequency-diffusion radiation transport in a way similar to those for the optically thin approximation presented above. The implementation of an expanded level structure in the model is necessary if the population densities of the lower states of each transition are to be determined accurately, self-consistently with other states of the heliumlike ion, as well as with the excited and ground states of neighboring ions.

As was mentioned, the line source function in an opaque plasma is attenuated by a factor dependent on the optical depth and on the mechanism by which the emission line is broadened. In this study, we have chosen to describe the optically thick line shape by a Voigt line profile, taking into account the collisional and radiative broadening of both the upper and lower levels comprising the transition of interest. At very high densities, Stark profiles are necessary to describe the line shape accurately. This problem is currently being addressed by Jacobs and Davis, but no profiles have been calculated as of this writing.

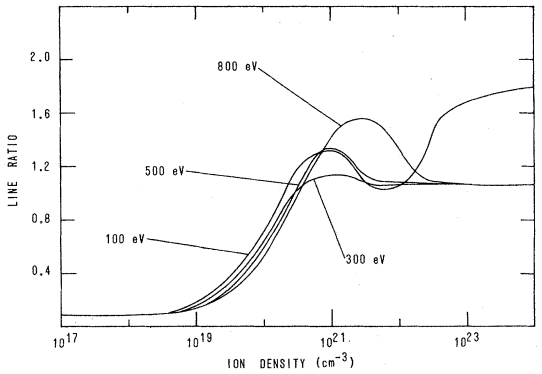

FIG. 5. $(1s2p\,^3P \rightarrow 2p^{2\,3}P)/(1s2s\,^3S \rightarrow 2s2p\,^3P)$ intensity ratio for a neon plasma of radius 100 μm—with opacity effects.

The results of the calculations with opacity effects included are presented in Figs. 5–7 for a neon, aluminum, and argon plasma, respectively. The studies were performed for plasmas with a radius of 100 μm over a range of ion densities and electron temperatures identical to those used for studying this line ratio in the optically thin approximation (Figs. 2–4).

Upon comparison of the three figures, certain aspects of the calculation for each different plasma are seen to be similar, and can be discussed in terms of a general plasma radiating in this temperature and density regime:

(i) The line ratio exhibits, initially, a decrease relative to the optically thin result, which occurs at an ion density somewhat higher than that at which departure from the coronal result takes place. Evidently, the $1s2p \rightarrow 2p^2$ line intensity must be affected by opacity at a lower density than the $1s2s \rightarrow 2s2p$ intensity, despite the fact that the former has an oscillator strength roughly two-thirds of the latter transition. This effect

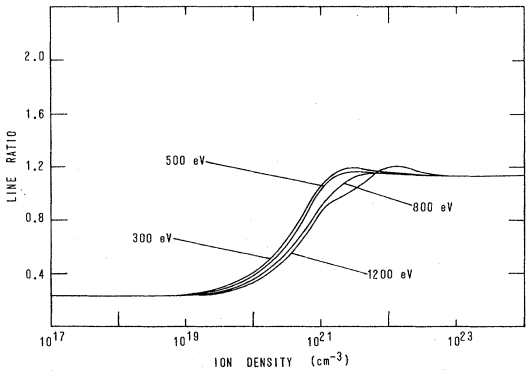

FIG. 6. $(1s2p\,^3P \rightarrow 2p^{2\,3}P)/(1s2s\,^3S \rightarrow 2s2p\,^3P)$ intensity ratio for an aluminum plasma of radius 100 μm—with opacity effects.

can be understood in terms of the lower-state population densities as determined by the collisional radiative model. At the densities at which the opacity effects first manifest themselves, the lower state of the former transition, the $1s2p\,^3P$ level, is more populated then the lower state of the other transition, the $1s2s\,^3S$ level, owing to the strong collisional mixing of these levels at these large electron densities. The ratio of the statistical weights is 3:1, but the ratio of these populations ranges, typically, from 2:1 to 3:1 above 10^{19} ions/cm^3, as is determined by the actual collisional and radiative rates employed in our model. Referring to Eq. (9), therefore, the optical depth at line center for the $1s2p \rightarrow 2p^2$ transition will be approximately 1.3–1.9 times greater than that of the $1s2s \rightarrow 2s2p$ transition, and, consequently, will experience photon reabsorption at a lower density, resulting in the initial decrease in the line ratio. Hence, accurate collisional and radiative rates are necessary for a model to accurately predict the ion density at which deviations from the optically thin approximation will first appear.

(ii) The line ratio will exhibit this initial decrease owing to opacity, in general, at a higher density for a higher-temperature plasma. For example, in Fig. 6, the aluminum plasma will yield a line ratio which begins to flatten out at 10^{21} ions/cm^3 for the 300-eV case, but this doesn't occur until 3×10^{21} ions/cm^3 for the 800-eV plasma. This effect is simply a manifestation of the ion temperature dependence of the optical depth, which can be seen, in Eq. (9), to fall off as $T_i^{-1/2}$. Deviations from this effect can occur at low temperature, however, as is seen in Fig. 5 for a neon plasma at 100 eV and in Fig. 7 for an argon plasma at 500 eV. The departure from the optically thin result occurs at higher densities than

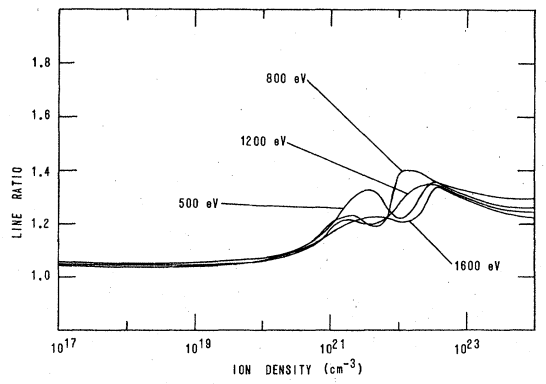

FIG. 7. $(1s2p\,^3P \rightarrow 2p^2\,^3P)/(1s2s\,^3S \rightarrow 2s2p\,^3P)$ intensity ratio for an argon plasma of radius 100 μm—with opacity effects.

it does for the higher-temperature plasmas. What is occurring at lower temperatures is a major change in the abundance of the heliumlike-ion populations. Over a wide range of temperature (at constant ion density) the heliumlike ion is the dominant ion population in the plasma[16]; hence the $1s2s\,^3S$ and $1s2p\,^3P$ densities will be large. At low temperatures, however, these densities fall rapidly, yielding to lower stages of ionization; consequently, the optical depths of the two transitions also decrease rapidly, delaying the onset of the opacity effects until higher densities, in spite of the lower-temperature plasma effect described above.

(iii) The line ratio will converge, at high densities, to an LTE limit significantly different from that predicted by the calculation when done in the optically thin approximation. Although the upper-state populations of the two transitions will eventually relax to the same LTE ratio (1:1) in the high-density limit regardless of the opacity effects (collision-dominated plasma regime), the radiation emission will be quite different from the optically thin prediction. This can be demonstrated by using an approximate analytic model,[15] in which the radiation is attenuated by a factor γ, where[17,18]

$$\gamma \propto (a/\tau_0)^{1/2}, \tag{11}$$

where a is the Voigt damping parameter, proportional to the sum of all collisional and radiative rates depopulating the upper and lower levels of the transitions. From Eq. (6) the LTE line ratio in the optically thick case now becomes

$$R_{\mathrm{LTE}}(\mathrm{thick}) = R_{\mathrm{LTE}}(\mathrm{thin})(\gamma_2/\gamma_1)\,. \tag{12}$$

Now, from Eq. (9), τ_0 is proportional to the oscillator strength and the lower-state densities, giving

$$\gamma_2/\gamma_1 = (a_2 f_1 N_{1s2s}/a_1 f_2 N_{1s2p})^{1/2}, \tag{13}$$

where

$$f \propto (g_u/g_l) A\lambda^2 \tag{14}$$

(u and l refer to upper and lower states) and, in the LTE limit,

$$N_{1s2s}/N_{1s2p} \cong g_{1s2s}/g_{1s2p}\,. \tag{15}$$

Noting that the wavelengths are approximately equal and inserting the appropriate statistical weights, one obtains

$$R_{\mathrm{LTE}}(\mathrm{thick}) = R_{\mathrm{LTE}}(\mathrm{thin})(a_2 A_1/a_1 A_2)^{1/2}\,. \tag{16}$$

At high densities, the parameter a is dominated by collisional rates; we have calculated the required electron-collisional excitation rates (de-

TABLE II. Electron collisional excitation and deexcitation rate coefficients which dominate the collision broadening of the satellite lines.

Transition		Neon (10^{-9})	Aluminum (10^{-9})	Argon (10^{-9})
300 eV	X	5.7	2.7	1.43
	Y	5.87	2.81	1.52
	x	7.7	3.5	0.463
	y	2.6	1.24	0.173
500 eV	X	4.53	2.13	1.14
	Y	4.61	2.18	1.18
	x	6.1	2.82	0.47
	y	2.1	9.65	0.168
800 eV	X	3.63	1.71	0.914
	Y	3.67	1.73	0.936
	x	4.87	2.27	0.460
	y	1.64	7.70	0.16

excitation is obtained by detailed balance) using our distorted-wave approximation,[12] and the dominant rates are those depicted in Fig. 1 as X, Y, x, and y and are listed in Table II. Over the range of temperatures studied here, the ratio a_2/a_1 is determined to be nearly constant at high densities (see Table II) with values of 0.63 for neon, 0.64 for aluminum, and 0.8 for argon. Using the values given in Table I and Eq. (16) we obtain, for the LTE line ratio in the optically thick case, 1.05 for neon, 1.105 for aluminum, and 1.2 for argon, which are seen to agree quite favorably with the model results in Fig. 5–7. Small discrepancies occur in the case of argon since (i) the ratio a_2/a_1 is not strictly constant with temperature owing to the dominance of the doubly excited-state mixing rates (see Table II), and (ii) the argon plasma has not yet reached a state of complete LTE at 10^{24} ions/cm^3 (see Fig. 7).

Although several features of the line ratio in the various plasmas are similar, there are still some contrasting features apparent in the optically thick results. The most obvious physical effect, although only a slight one, is the increase in the density at which opacity effects occur with atomic number Z, as seen in Fig. 5–7. This finds explanation in the actual scaling of electron collisional excitation rate coefficients, which decrease in magnitude at threshold with Z. A decrease in the populating rates at a given density corresponds to a decrease in excited-level densities and, consequently, the optical depths of the transitions of interest here. Thus at 10^{21} ions/cm^3 and a nominal electron temperature of 800 eV, the $1s2p\,^3P$ state of aluminum will be more populated than the same state of a similar argon plasma. Hence, the optical depth of the $1s2p\,^3P \rightarrow 2p^2$ transition will be "thicker" in the aluminum plasma than in the argon plasma, and opacity effects will occur at a lower density.

In Fig. 5, the optically thick line ratio for the neon plasma at 100 eV displays rather anomalous behavior at high densities. What is occurring here is a high-density effect decreasing the abundance of the heliumlike neon ion until the satellite lines are no longer optically thick and the ratio rises to its optically thin LTE limit, an effect similar to the one described earlier due to low plasma temperature. Simply stated, an increase in ion density at constant temperature usually drives a plasma toward a state of lower ionization.[16] Once again, the heliumlike ion, owing to its "closed-electron-shell" configuration, maintains a relatively large population density over a wide range of densities. However, at high enough densities, particularly at low temperatures, the ion abundance shifts toward lower charge states rapidly, generating a corresponding drop in excited-state populations and resulting in a line-ratio behavior as seen in Fig. 5. The same behavior would be seen for aluminum and argon if curves for lower temperatures had been of interest in this work. However, the onset of this behavior in a laboratory plasma would usually be accompanied by a significant decrease in the line intensities, making this diagnostic inaccurate at these densities due to its weak appearance in the spectra.

The most striking difference between the optically thick results for the three plasmas, however, is seen as a single shoulder or "hump" in neon, the absence of a shoulder in aluminum, and a double shoulder in argon. Although many factors affect the line-ratio behavior as have been discussed in detail above, the Z scaling of the value of the LTE optically thick limit and the density at which LTE is reached are most important

in determining this shape. For the argon plasma, in Fig. 7, the "double hump" occurs as, first, the $1s2p \rightarrow 2p^2$ intensity is attenuated by opacity, decreasing the ratio; second, the $1s2s \rightarrow 2s2p$ transition becomes thick, attenuating that line intensity and thus increasing the ratio; third, the plasma becomes collision dominated, the line ratio tends toward its LTE limit, *and* this limit is lower than the value the ratio has attained before entering the LTE regime, causing the ratio to decrease and creating the second hump. In the aluminum plasma in Fig. 6, LTE is reached before the second shoulder can manifest itself, and the LTE value for the ratio is approximately *equal* to the value the ratio has attained before LTE is reached, allowing for only a very mild shoulder structure, most apparent at 1200 eV. For the neon plasma, in Fig. 5, the LTE state is also reached at relatively lower densities, but the LTE value of the line ratio is much *lower* than the value the ratio has attained before entering the LTE state, hence a single pronounced "hump" is evident.

Since the occurence of these shoulders and the value of the LTE limit of the line ratio seem to be strongly dependent on the actual atomic parameters of the particular plasma of interest, prediction of a general shape would seem difficult in light of the many ways the parameters in Table I scale with Z. Unfortunately, this seems to indicate that each element requires, to a certain extent, individual treatment if this line ratio is to be applied successfully to diagnose laboratory plasmas in which photoexcitation is an important process.

IV. DISCUSSION

We have studied the heliumlike-satellite line-intensity ratio with our sophisticated collisional-radiative ionization-dynamics model in order to assess, within the context of an optically thick plasma, the value of this ratio as a plasma density diagnostic in the high-density, high-temperature plasma regime encountered in recent laser-pellet interaction experiments. The behavior of the line ratio was first examined under the assumption of an optically thin plasma. It was found that the density profile of the line ratio was independent of ion-state populations in this approximation. In addition, it was found that the density-sensitive range of the line ratio occurred at higher densities with increasing atomic number, extending the range of applicability of this diagnostic, depending on the choice of the fill gas. The results were compared with other independent work and with limiting values determined from simple analytic models, and in all cases the agreement was quite favorable.

Armed with confidence in the model and understanding gained from the optically thin analysis, we proceeded to investigate the effects of stimulated absorption and emission on these plasmas by "turning on" the opacity calculation. The most obvious result from this study was that, indeed, the satellite-line ratio from plasmas of this type was affected by opacity, despite the fact that the lower levels of the two transitions are excited states of the heliumlike ion. Not only did the deviations from the optically thin result occur at densities where the diagnostic is most sensitive and useful, but many of the line ratios were multiple valued with density, making accurate diagnostics difficult. As further analysis illustrated, the actual shape and overall behavior of the line ratio versus density was a sensitive function of the atomic parameters pertaining to the individual plasma. This finding led to two inescapable conclusions: (a) accurate theoretical modeling of this diagnostic in the "thick" case depends on a comprehensive level structure within the CRE model and accurately determined cross sections characterizing the collisional processes linking the level structure, and (b) owing to the complex interaction of the various atomic parameters in determining the level populations and radiation field, and the various Z dependencies of these parameters, simple Z scaling of the line-ratio behavior in a reabsorbing plasma is not likely; rather, each plasma will have to be characterized individually.

In light of the results obtained for the intensity ratio with photoexcitation processes included in the calculation, it would appear that opacity effects may cause some departure from optically thin results at densities presently encountered in pellet-fusion experiments. The extent of this departure, of course, will depend on the initial fill pressure of the admixture. By using very low fill pressures, the density of the additive gas at peak compression will be below the density at which opacity effects commence to affect the ratio; however, the trade-off is in the reduced number of emitting ions, resulting in emission lines with intensities which may be too low to measure accurately with existing spectroscopic methods.

To determine the degree of the self-absorption effects in typical microballoon experiments, a parameter study has been done for neon and argon where the source size has been scaled with the density as $N^{-1/3}$. Plasma radii were determined by using the law of mass conservation and a set of initial conditions chosen to model actual micro-

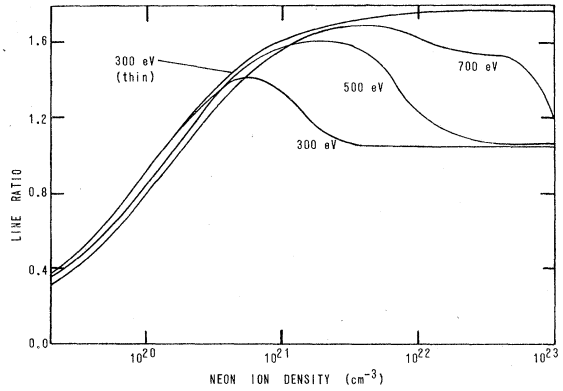

FIG. 8. $(1s2p\,^3P \rightarrow 2p^2\,^3P)/(1s2s\,^3P)$ intensity ratio for a neon plasma corresponding to initial conditions of a 180-μm-diam microballoon with 1 atm of neon and 9 atm of DT.

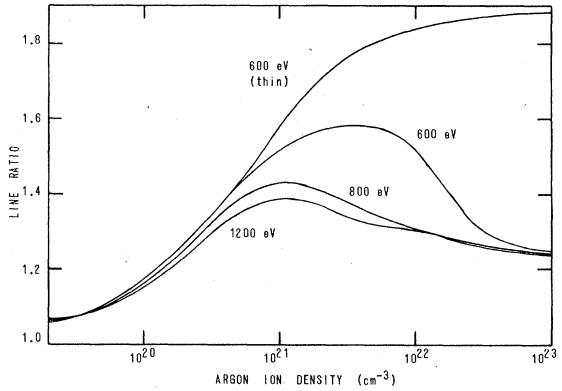

FIG. 9. $(1s2p\,^3P \rightarrow 2p^2\,^3P)/(1s2s\,^3S \rightarrow 2s2p\,^3P)$ intensity ratio for an argon plasma corresponding to initial conditions of a 230-μm-diam microballoon with 0.4 atm of argon and 30 atm of DT.

balloon experiments. For the neon study, a balloon diameter of 180 μm and fill pressures of 1 atm of neon and 9 atm of deuterium-tritium (DT) (10% neon gas, by volume) were chosen as typical initial conditions.[5] The argon study was modeled after recent experiments[19] which employed 230-μm-diam glass shells with fill pressures of 0.4 atm of argon and 30 atm of DT. While the DT gas does not affect the neon satellite-line radiation directly, the increase in electron density due to the ionization of the DT atoms will affect the collisional dynamics which determine the level populations of the impurity ions, and must be taken into account. This results in an increase in the electron density by factors of approximately 2 and 7 for neon and argon, respectively, compared to that of the seed gas alone at the temperatures for which the study was done.

In Fig. 8, the results of the neon study are shown for electron temperatures of 300, 500, and 700 eV, along with the optically thin result at 300 eV plotted versus neon-ion density. Similarly, the argon results at 600, 800, and 1200 eV with an optically thin curve for 600 eV are shown in Fig. 9 versus argon-ion density. The effect of photoexcitation is seen to cause departure from the thin result at implosion diameters of between 20 and 30 μm in the case of neon and at a diameter of about 45 μm for argon, representative in both cases of compression volumes attainable by existing systems. Clearly, the optically thin results are not accurate at higher compressions.

The final point of this discussion which we would like to emphasize is the necessity for comprehensive, detailed calculations of spectral signatures when attempting to determine parameters from these laboratory plasmas. Opacity effects on the radiation emission need not render the spectrum useless for diagnostic purposes; multivaluedness, as seen in Fig. 8 and 9, need not mitigate line-intensity ratios for applicability in deciphering the plasma-radiation signature. No single density or temperature indicator should be relied on, but rather, searching for consistency among several radiation diagnostics in the spectrum is required in order to draw accurate conclusions regarding the general plasma state.

ACKNOWLEDGMENTS

This work was supported by the Defense Nuclear Agency. One of us (D. D.) was supported by an NRC-NRL Resident Research Associateship.

*Present address: Science Applications, Inc. McLean, Va. 22101.

[1]D.J. Nagel, P. G. Burkhalter, C. M. Dozier, J. F. Holzrichter, B. M. Klein, J. M. MacMahon, J. A. Stamper, and R. R. Whitlock, Phys. Rev. Lett. 33, 743 (1974).

[2]P. G. Burkhalter, J. Davis, J. Rauch, W. Clark, G. DalBaca, and C. Stallings, J. Appl. Phys. 50, 705 (1979); P. G. Burkhalter, C. M. Dozier, and D. J. Nagel, Phys. Rev. A 15, 700 (1977).

[3]P. G. Burkhalter, J. Shiloh, A. Fisher, and Robert D. Cowan, J. Appl. Phys. 50, 4532 (1979).

[4]B. Yaakobi, D. Steel, E. Thorsos, A. Hauer, and B. Perry, Phys. Rev. Lett. 39, 1526 (1977).

[5]K. B. Mitchell, D. B. van Hulsteyn, G. H. McCall, Ping Lee, and H. R. Griem, Phys. Rev. Lett. 42, 228 (1979).

[6]Hans R. Griem, Milan Blaha, and Paul C. Kepple,

Phys. Rev. A 19, 2421 (1979).
[7]J. Davis, NRL Memorandum Report 2655, October 1973 (unpublished).
[8]A. V. Vinogradov, I. Yu. Skobelev, and E. A. Yukov, Sov. J. Quantum Electron. 5, 630 (1975).
[9]A. V. Vinogradov, I. Yu. Skobelev, and E. A. Yukov, Sov. Phys. JETP 45(5), 925 (1977); I. Yu. Skobelev, A. V. Vinogradov, and E. A. Yukov, Phys. Scr. 18, 78 (1978).
[10]John F. Seely, Phys. Rev. Lett. 42, 1606 (1979).
[11]L. A. Vainshtein and U. I. Safronova, At. Data Nucl. Data Tables 21, 50 (1978).
[12]J. Davis, P. C. Kepple, and M. Blaha, J. Quant. Spectrosc. Radiat. Transfer 16, 1043 (1976).
[13]J. Richter, in *Plasma Diagnostics*, edited by W. Lochte-Holtgreven (North-Holland, Amsterdam, 1968).
[14]R. W. P. McWhirter, in *Plasma Diagnostic Techniques*, edited by R. H. Huddlestone and S. L. Leonard (Academic, New York, 1965).
[15]D. Duston and J. Davis, NRL Memorandum Report 3846, September 1978 (unpublished).
[16]D. Duston and J. Davis, Phys. Rev. A (to be published).
[17]R. G. Athay, *Radiation Transport in Spectral Lines*, (Reidel, Dordrecht, Holland, 1974), Chap. 2.
[18]J. P. Apruzese, J. Davis, and K. G. Whitney, J. Quant. Spectrosc. Radiat. Transfer 17, 557 (1977).
[19]A. Hauer (private communication).